Appl. Phys. B (2014) 114:275–281
DOI 10.1007/s00340-013-5688-7

Applied Physics B
Lasers and Optics

Long-term drifts of stray electric fields in a Paul trap

A. Härter · A. Krükow · A. Brunner · J. Hecker Denschlag

Received: 29 May 2013 / Accepted: 8 October 2013 / Published online: 7 November 2013

Abstract We investigate the evolution of quasi-static stray electric fields in a linear Paul trap over a period of several months. Depending on how these electric fields are initially induced, we observe very different timescales for the field drifts. Photo-induced electric fields decay on timescales of days. We interpret this as photo-electrically generated charges on insulating materials which decay via discharge currents. In contrast, stray fields due to the exposure of the ion trap to a beam of Ba atoms mainly exhibit slow dynamics on the order of months. We explain this observation as a consequence of a coating of the trap electrodes by the atomic beam. This may lead to contact potentials which can slowly drift over time due to atomic diffusion and chemical processes on the surface. In order not to perturb the field evolutions, we suppress the generation of additional charges and atomic coatings in the Paul trap during the measurements. For this, we shield the ion trap from ambient light and only allow the use of near-infrared lasers. Furthermore, we minimize the flux of atoms into the ion trap chamber. Long-term operation of our shielded trap led us to a regime of very low residual electric field drifts of less than 0.03 V/m per day.

A. Härter · A. Krükow · A. Brunner · J. Hecker Denschlag (✉)
Institut für Quantenmaterie and Center for Integrated Quantum Science and Technology (IQST), Universität Ulm, 89069 Ulm, Germany
e-mail: johannes.denschlag@uni-ulm.de

Present Address:
A. Brunner
Universität Stuttgart, 3. Physikalisches Institut, 70569 Stuttgart, Germany

1 Introduction

Paul traps have become essential tools in widely different fields of research ranging from quantum information [1–3] and quantum simulation [4] to precision metrology [5] and cold collisions between ions and neutrals [6–11]. The further development of all these lines of research hinges on continuing improvements of the Paul trap architectures and on a better understanding of the current experimental issues.

Ideally, a single ion in a Paul trap is only subjected to the electric fields generated by the voltages applied to the trap electrodes. However, even small spatial variations of the electrode surface potential (i.e. patch potentials) in the vicinity of the trap center create stray electric fields that significantly perturb this ideal configuration. This leads to undesired experimental complications. Quasi-static stray fields lead to positional shifts of the trapped ion [12–19] and thus to excess micromotion [20]. Rapidly fluctuating stray fields lead to ion heating [15–18, 21–25].

For the following discussion, we will formally group patch potentials into two categories.

Patch potentials of category 1 can decay via electronic discharge currents, similar to a capacitor that is shorted with a resistor. Thus, their evolution is in general governed by the motion of electrons. For example, the photoelectric effect can generate charges on the dielectric surfaces of the Paul trap. These surfaces could be the trap mounts but also insulating oxide layers on the trap electrodes. The photoelectric effect typically appears with light at wavelengths below about 500 nm. As most of the trapped ion species require light at such "blue" wavelengths for laser cooling and interrogation, light-induced patch charges will continuously be created while the experiments are carried out. In addition, patch potentials of category 1 can also be

generated in other ways such as the direct deposition of electrons and ions on dielectric surfaces (see e.g. [14]).

Patch potentials of category 2 are stable as long as the surface atoms do not move. They are due to a spatial variation of the material's work function which depends on its composition, its crystal orientation, and its surface adsorbates [26, 27]. Surface adsorbates can be elements or compounds which are physically or chemically bound onto the surface. Crystal orientation comes into play for neighboring grains in a polycrystalline structure. A change in composition comes about, e.g. when two different metals are brought into contact. This gives rise to the contact potential, i.e. the difference of the work functions of the two metals. Ion traps are often loaded from atomic beams that are directed toward the trap center. If the atomic beam hits the Paul trap electrodes, atoms are deposited on the electrode surface, potentially forming contact potentials. Furthermore, as previously mentioned, the formation and deposition of chemical compounds on the trap surface can also create electric stray fields.

Patch potentials of both categories have been observed to cause deteriorations of Paul traps leading to strong ion heating effects [15–17, 21–25]. However, the influence and evolution of the patch potentials of category 2 was often masked by the presence of photo-induced patch potentials.

Here, we study the long-term dynamics of quasi-static electric fields in a Paul trap in an environment where we systematically suppress both continuous surface contamination and continuous photo-induced patch charge buildup. We observe smooth drifts of the quasi-static electric stray fields on various timescales from days to months. We interpret these different timescales as indications of different physical and chemical processes that take place. For example, electric fields induced by the exposure of the trap to laser light typically decay within a few days. Fields induced by creating an atomic beam using a barium oven show slower dynamics on the order of months. After longer time periods without surface contamination and photo-induced charging, the stray electric fields settle smoothly toward a stable value with very small residual drifts as low as 0.03 V/m per day.

In our setup, we achieve the suppression of surface contamination and photo-induced patch charges as follows. We create and probe ions (Rb^+) in a linear Paul trap by using only near-infrared light sources (λ = 780 and 1,064 nm) and small clouds of $\approx 10^5$ ultracold Rb atoms, which have previously been optically transported into the chamber [28]. Thus, the net flux of atoms into the chamber is negligible. We measure the electric stray fields by applying compensating electric fields until the excess micromotion of the ion is minimized [29].

2 Experimental setup and methods

The design of our linear Paul trap is shown in Fig. 1. The effective distance from the trap center to each of the four radiofrequency (rf) electrodes is 2.6 mm, while the distance to the endcap electrodes measures 7 mm. To create radial confinement, a voltage driven at a frequency of 4.17 MHz with an amplitude of 500 V is applied to two of the rf electrodes while the other two are held at ground potential. Axial confinement is generated by applying static voltages of about 8 V to the two endcap electrodes. Under these experimental conditions, an $^{87}Rb^+$ ion is confined at radial trapping frequencies of about 350 kHz and an axial trapping frequency of about 50 kHz. The total depth of the trap is on the order of 4 eV and allows for ion storage times of many days, even without any type of cooling. The Paul trap is part of a hybrid atom-ion trap setup that brings the trapped ion into contact with an ultracold cloud of atoms [30]. Ensembles of ^{87}Rb atoms are prepared in a separate vacuum chamber and transported into the Paul trap using a long-distance optical transport line. They are then loaded into a crossed dipole trap where further evaporative cooling down to typical temperatures of 700 nK is performed. The atom numbers typically range between 10^5 and 10^6 atoms. Both the optical transport and the crossed dipole trap are implemented using several W of laser power at a wavelength of 1,064 nm. To perform absorption imaging of the atoms, resonant laser light at 780 nm is used. After this destructive imaging process, a new atom cloud is prepared within 30 s for the next measurement. To load an ion, a Rb atom cloud with a density of several 10^{13} cm^{-3} is prepared and positioned at the center of the Paul trap. Three-body

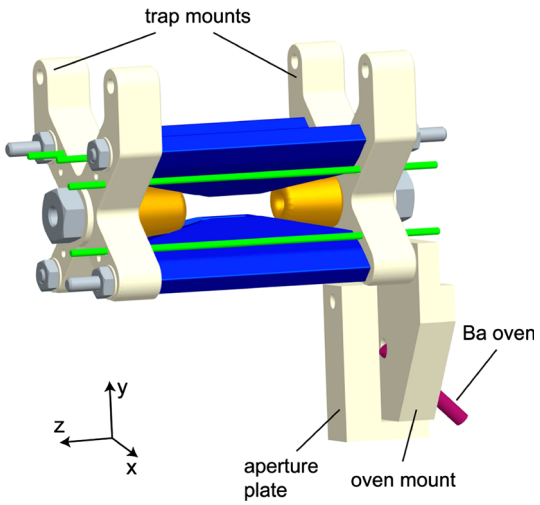

Fig. 1 Paul trap with mounts. The trap consists of four rf electrodes (*blue*), two endcap electrodes (*yellow*), and two pairs of compensation electrodes (*green*). The mounts for the trap and the barium oven are made of MACOR. The aperture plate was installed to reduce the amount of barium deposited on the trap electrodes

recombination processes in the atom cloud produce Rb_2 molecules that are subsequently ionized by a REMPI process using photons from the dipole trap laser [28]. Subsequently, the molecular Rb_2^+ ions quickly dissociate via collisions with neutral atoms and finally yield Rb^+ ions.

To detect the number of trapped Rb^+ ions and measure their micromotion, we employ a sensitive probing scheme using ultracold atomic clouds [29]. For this, we immerse the ions into clouds consisting of about 10^5 atoms at densities around 10^{12} cm^{-3}. After a few seconds of interaction time, we detect the final atom number and atom temperature which depend on the number of ions and their micromotion. This enables us to reliably work with a single ion and, by minimizing its excess micromotion with the help of electric compensation fields, to measure the stray electric fields acting on the ion [20, 29]. Due to the production time required for the atom clouds, an electric field measurement requires about an hour of measurement time, resulting in a limited temporal resolution. The measurement precision is high and typically ranges around 0.1 V/m for the results presented here.

3 Results

As a first step, we investigate the susceptibility of our trap setup with respect to laser light at various wavelengths that are available in our laboratory (Fig. 2). For these and the following measurements, each laser beam propagates through the center of the ion trap in horizontal direction at an angle of 45° with respect to the trap axis. In particular, the laser beam and its specular reflection from the vacuum windows do not directly impinge on any trap electrode or trap mount. Only some stray scattered light from the windows illuminates the trap parts diffusely and quite evenly. Both the trap electrodes and the trap mounts can be "charged up" via the photoelectric effect. The trap mounts and the mounts for the barium oven are made of machinable glass-ceramic (MACOR), which is very susceptible for accumulating charges. Charges can also accumulate on the trap electrode surfaces as these often feature undesired insulating coatings such as oxide layers. As expected, for wavelengths below 500 nm, we find a sharp increase in light-induced buildup of electric fields (see Fig. 2). For 780 nm or the even longer wavelength of 1,064 nm, we did not detect any measurable light-induced electric fields.

In general, we find the photo-induced stray electric fields to be pointing mostly in vertical ($+y$-axis) and axial ($+z$-axis) direction. There might be a number of reasons how this asymmetry in the direction of the electric stray field comes about. One reason could be that the laser light illuminates the trap setup asymmetrically. However, we can exclude this possibility as the field direction is quite

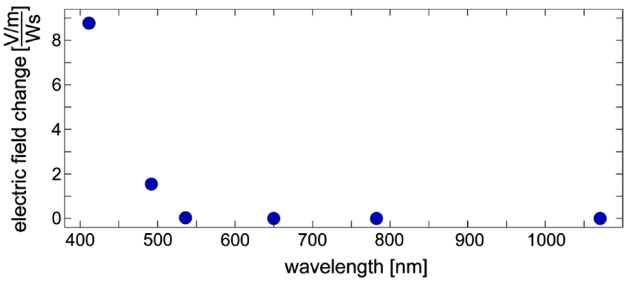

Fig. 2 Changes of the *vertical* stray electric field normalized to laser power and exposure time. The field changes were observed to be linear in both laser power and exposure time. At wavelengths below 500 nm, light-induced electric fields sharply increase

insensitive to changes in the propagation direction of the laser light, in particular when it is flipped by 90° in the horizontal plane. Another possible explanation for the asymmetry could be the presence, e.g. of a single dust particle on the trap electrodes, which is something we cannot rule out. An obvious asymmetry, however, is already inherent in our Paul trap setup due to the location of the mount and aperture plate of the barium oven (see Fig. 1, lower right). Indeed, we estimate that these two parts (which are made of MACOR) can lead to significant electric stray fields at the location of the ion. For one, they can potentially be charged to voltages of up to 500 V, as determined by the amplitude of the rf trap drive. (The rf fields prevent the patch potentials from saturating at a low voltage, the value of which would be normally set by the difference of the work function and the photon energy.) Secondly, our trap geometry is relatively open such that external electric fields can penetrate quite well to the position of the ion. We cannot deterministically charge the aperture plate or the oven mount to a certain voltage in order to test their effect on the electric field at the position of the ion. However, we can apply voltages to the Ba oven itself which should create electric fields of similar magnitude and orientation. We find that a voltage of 1 V on the oven indeed results in a dominant electric field contribution of $+0.1$ V/m in y-direction. The other two field components are each about a factor of 6 smaller (-0.016 V/m in x-direction and $+0.016$ V/m in z-direction). These values set a lower bound to the expected fields originating from a charged aperture plate which is located closer to the ion than the oven.

Next, we start a long-term experiment where we monitor the evolution of all three spatial components of the stray electric field over a time span of about 4 months (Fig. 3). Before the start of these measurements, the ion trap was operated with Ba^+ ions so that both the barium oven and the necessary lasers were frequently used. Consequently, there is a substantial stray electric field to begin with. During the measurements (except for two short occasions),

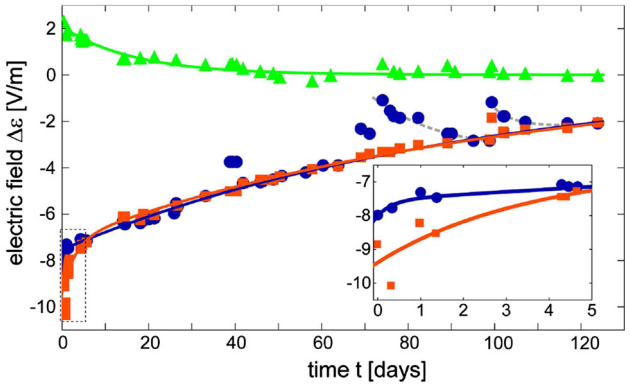

Fig. 3 Long-term drift of the *horizontal* (*x*-direction, *orange squares*), *vertical* (*y*-direction, *blue circles*), and axial (*z*-direction, *green triangles*) electric fields. Except for two occasions ($t \approx 70$ and $t \approx 100$ days), the trap was isolated from any light below a wavelength of 780 nm. *Solid lines* are double-exponential fits with long-term time constants on the order of 3 months. Offsets of the electric fields are chosen such that $\Delta\varepsilon$ converges toward 0 in the long-term limit. *Inset* zoom into the initial field evolution with time constants of 0.3 and 2.7 days (cf. Table 1)

the whole experimental setup is almost entirely shielded from ambient light by means of light-tight protective covers to avoid any patch charge buildup. All three electric field components (in *x*-, *y*-, *z*-direction) show a more or less monotonic decay and converge toward long-term limits which are each set to $\Delta\varepsilon = 0$ in the plot. The solid lines in Fig. 3 are double-exponential fits of the form

$$\varepsilon(t) = \Delta\varepsilon_1 \exp(-t/\tau_1) + \Delta\varepsilon_2 \exp(-t/\tau_2),$$

where $\Delta\varepsilon_{1,2}$ are the electric field shifts and $\tau_{1,2}$ are the time constants of the exponential decay curves. For the two radial directions (*x*- and *y*-directions), we find relatively rapid initial decays with time constants τ_1 = 0.3–2.7 days (see inset of Fig. 3) and subsequent slow decays with $\tau_2 \approx 90$ days. In axial direction, the time constants are 0.6 and 18 days. For all three directions, the slow decays are dominant as they account for roughly 80–95 % of the electric field shifts (see Table 1).

On two occasions ($t \approx 70$ and $t \approx 100$ days), the light-tight protective covers around the experimental setup had to be removed for several hours so that the Paul trap was subjected (quite uniformly) to ambient white light from the fluorescent ceiling lights. As a consequence, the electric field in vertical (*y*) direction shows a sharp increase and then decays back toward its long-term behavior within several days. We investigate this effect in detail below.

After about 100 days, the daily drift of the vertical field was below 0.03 V/m yielding extremely stable experimental conditions. In addition, this slow drift allows for a precise prediction of the expected electric fields at a given time so that the field compensation can be adjusted without requiring additional measurements.

After the time period shown in Fig. 3, we make use of the low stray field drift to selectively test the dynamics of photo-induced patch charges. For this measurement, we shine through the chamber about 2.5 mW of laser power at a wavelength of 413 nm (3 eV) for 4 min. The direction of the laser beam and the conditions with respect to trap illumination are the same as for the measurements in Fig. 2, as discussed in the beginning of Sect. 3. The strongest effect is again observed in the vertical electric field component which increases by about 6 V/m. The axial field component increases by 1.5 V/m, and the horizontal component increases by 0.6 V/m. The laser was then switched off and the decay of the vertical field component was monitored over 5 days (Fig. 4). The data are fit by a double-exponential curve with an initial decay on a timescale $\tau_1 = 1.2$ days and a slow decay with $\tau_2 = 11$ days. This slow decay accounts for about 80 % of the field shift. The observed initial increase and subsequent decay of the electric field are in rough agreement with the behavior seen in Fig. 3 after the Paul trap had been subjected to ambient light. Thus, our data in Figs. 3 and 4 clearly indicate that photo-induced electric fields decay on typical timescales of a few days.

We explain the evolution of the photo-induced stray fields as follows: Initially, the photoelectric effect generates charges on electrically isolated surfaces resulting in electric stray potentials. Over time these potentials discharge by the finite resistivity of the material. In case of a charging of the aperture plate or the oven mount, we can estimate a timescale for the discharge. At room temperature, MACOR has a specific volume resistivity of about $10^{17}\,\Omega\,\mathrm{cm}$. The typical resistance of a cm-sized component then is on the order of $10^{17}\,\Omega$. The electric capacitance of a cm^2-sized plate is about $4\varepsilon_0$ cm, with ε_0 denoting the vacuum permittivity. Thus, the decay constant is on the order of 10 h, which roughly agrees with our observed timescales. We note that the resistivity of MACOR is strongly temperature dependent. We do not have a precise knowledge of the temperature of the mount but from our estimate it is clear that timescales for the discharging of the MACOR parts should not be much longer than a few days. The fact that we observe not only a single timescale for the field decay indicates that there is more than one contribution to the stray fields. A charged up MACOR part might exhibit a different discharge behavior than a dust particle or an isolated patch on the electrode surface. In any case, the data in Fig. 4 and especially in Fig. 3 (at $t \approx 70$ and $t \approx 100$ days) clearly indicate that photo-induced fields always decay on a timescale faster than 2 weeks. The question is then how the very slow drift taking place over about 90 days can be explained (see Fig. 3). Our observations suggest that the electric fields linked to this slow decay have a different origin than the photoelectric effect.

Table 1 Overview of the observed drift time constants and the corresponding electric field shifts

Direction	Cause	τ_1 (days)	$\Delta\varepsilon_1$ (V/m)	τ_2 (days)	$\Delta\varepsilon_2$ (V/m)
Vertical (Fig. 3)	Blue light + oven operation	0.3 ± 0.4	-0.4 ± 0.2	90 ± 10	-7.4 ± 0.4
Horizontal (Fig. 3)	Blue light + oven operation	2.7 ± 0.8	-2.1 ± 0.3	94 ± 21	-7.3 ± 0.7
Axial (Fig. 3)	Blue light + oven operation	0.6 ± 0.8	0.4 ± 0.2	18 ± 3	1.9 ± 0.1
Vertical (Fig. 4)	Blue light	1.2 ± 0.1	1.2 ± 0.1	11 ± 0.3	4.9 ± 0.1

Oven-induced and light-induced effects give rise to drifts with opposite signs

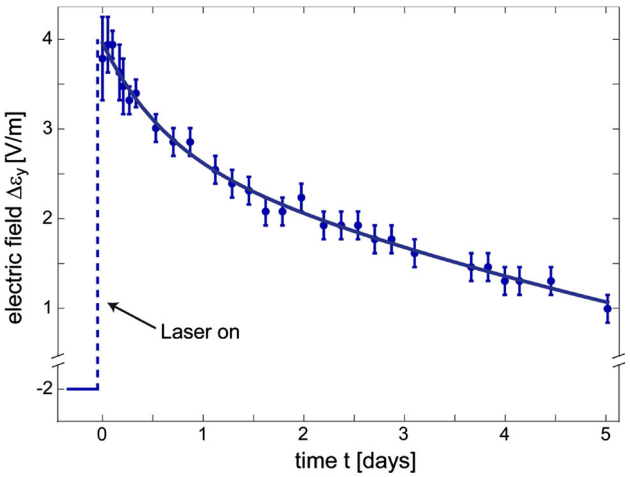

Fig. 4 *Vertical* electric field shift induced by subjecting the Paul trap to light at 413 nm. The subsequent relaxation is fit by a double-exponential function with a dominant slow decay accounting for 80 % of the field shift. The corresponding time constant is $\tau_2 = 11$ days

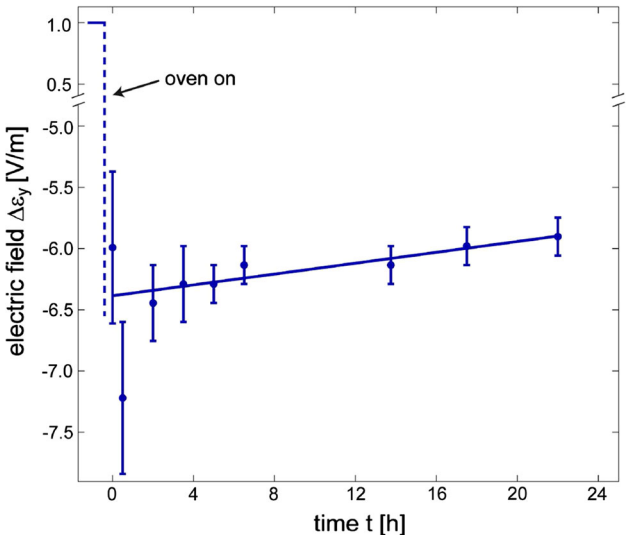

Fig. 5 *Vertical* electric field shift induced by heating the barium oven for 10 min. During the oven heating time, the field dropped by about 7.5 V/m. After the oven was turned off, the field shows a drift toward higher values. The *straight solid line* is a guide to the eye

We conjecture that the slow drifts originate from the dynamics of potentials of category 2, e.g. contact potentials. These potentials may change due to slow chemical reactions in the ultrahigh vacuum environment or by diffusion and migration processes on the electrode surface. It is known that barium reacts and forms compounds with O_2, N_2, CO_2, and H_2O. It also acts as a getter material, inclosing non-reactive gases. Thus, the mobility of Ba on a surface is sizeable. (Interestingly, the work function of barium is known to remain quite constant ($\approx$2.5 eV) even when contaminated with other substances.) Diffusion or migration of barium on the electrode surface can coat certain compound layers and set other ones free—thus giving rise to slowly changing contact potentials. At room temperature, the vapor pressure of barium is very low. Even at 200 °C, it only reaches 10^{-12} mbar. This suggests that barium coatings have a long lifetime at ambient temperatures. Previous studies have investigated the influence of barium contaminations on Paul trap electrodes made of Be–Cu [16]. Long timescales for the quasi-static electric stray field drifts on the order of months were found, similar to our time constant for the slow drift ($\tau_2 = 90$ days) in Fig. 3. Furthermore, it was found in [15] that baking out a Paul trap with tungsten electrodes that had been coated with Ba significantly changed electric stray fields.

In order to test our conjecture, we now investigate the influence of the barium oven (while keeping any light below a wavelength of 780 nm blocked off). Immediately after the measurements of Fig. 4 are completed, the oven is heated to a temperature of more than 600 °C for 10 min inducing a drop of the vertical electric field component by about 7.5 V/m (Fig. 5). The horizontal and axial fields each drop by about 2 V/m (not shown). This electric field drop may be partially explained by a rapid discharging of left-over light-induced charges on the oven mount caused by the heat dissipated by the oven. The conductivity of MACOR increases by more than ten orders of magnitude when heated from room temperature to several 100 °C. It can thus be expected that any leftover charges in the vicinity of the oven will be efficiently removed at such high temperatures. However, the electric field $\Delta\varepsilon$ drops much further than the initial value of -2 V/m in Fig. 4, namely down to -6.5 V/m. This additional negative electric field

drop cannot be explained by the discharge of the charges that were previously produced photoelectrically.

One possible explanation for this field contribution is the effect of contact potentials on the trap electrodes. Despite the collimation of the atomic beam through the aperture plate, a fraction of the atoms emerging from the barium oven reaches the rf electrodes close to the trap center. Such a coating of the electrodes might immediately change the distribution of the contact potentials in close vicinity to the ion. These potentials can be up to about a couple of Volts (V), as determined by the difference in work function of the metals involved. In our setup, there is a clear asymmetry on how the Ba oven may coat the trap electrodes with Ba atoms. The two lower rf electrodes will each be coated only on one side, whereas the two upper electrodes will probably be coated over the full tip. It is then to be expected that contact potentials of the upper electrodes dominate over the potentials of the lower ones. As the work function of Ba is lower than that of stainless steel, an electric field component should build up which points toward the negative y-axis. This is indeed what we observe. Furthermore, there is also an asymmetry in z-direction, as the atomic beam from the oven passes at an angle of about 45° through the blades (see Fig. 1). This may give rise to an electric stray field component in z-direction.

Figure 5 shows that after the oven is turned off, the vertical electric field component increases by about 0.5 V/m per day. Such a behavior agrees with the observations at the beginning of the long-term measurements shown in the inset of Fig. 3. This again supports our interpretation that the 90-day long drift behavior of the electric field in Fig. 3 is a result of initially coating the trap electrodes and mounts with Ba which afterward migrates and undergoes chemical reactions on the surface.

4 Conclusion

In conclusion, we have investigated the long-term drifts of quasi-static electric stray fields in a linear Paul trap. We find drifts on timescales ranging from about half a day to 3 months. We suggest that these different timescales reflect different physical or chemical processes. Light-induced electric fields decay on relatively short timescales on the order of a few days. This is most probably due to charges located on insulating material which slowly discharge via the high electric resistance. In contrast, electric fields which are induced by turning on the Ba oven exhibit long-term drifts on timescales of up to 90 days. Guided by analysis, our interpretation is that the oven coats the trap electrodes or mounts. As a consequence, contact potentials appear which give rise to the electric fields. These fields show long-term drifts possibly due to slow migration or reaction processes taking place on the electrode surface.

Patch potentials have been identified as the common source of both quasi-static and fluctuating electric fields. The timescales for the drifts and fluctuations of these fields is reflected by the dynamics taking place on different length scales of the patches. It has been found that atomic contamination of Paul traps lead to both quasi-static and rapidly fluctuating patch fields [14, 17, 16]. Our findings on the evolution and the origins of quasi-static charges may thus provide new insights into mechanisms connected to rapidly fluctuating charges such as anomalous heating effects. The results presented here are a first investigation with our setup in the direction of surface dynamics of patch potentials. In the future, the experiments can easily be refined to obtain more detailed information and to test hypotheses. For example, by locally applying laser fields on trap mounts and electrodes (either to heat them up or to produce photo-induced patch charges in a controlled way), we should be able to spatially probe surface properties. Another result of our work is that by systematically avoiding the creation of electric patch potentials, we are able to get into a regime of very small and predictable electric stray field drifts as low as 0.03 V/m per day. Such stability of the trap conditions may prove valuable for the future development of precision ion trap experiments.

Acknowledgments The authors would like to thank Stefan Schmid and Wolfgang Schnitzler for help in the laboratory. This work was supported by the German Research Foundation DFG within the SFB/TRR21.

References

1. D. Leibfried, R. Blatt, C. Monroe, D.J. Wineland, Rev. Mod. Phys. **75**, 281 (2003)
2. R. Blatt, D. Wineland, Nature **453**, 1008–1015 (2008)
3. H. Häffner, C. Roos, R. Blatt, Phys. Rep. **469**, 155–203 (2008)
4. R. Blatt, C.F. Roos, Nat. Phys. **8**, 277–284 (2012)
5. T. Rosenband, D.B. Hume, P.O. Schmidt, C.W. Chou, A. Brusch, L. Lorini, W.H. Oskay, R.E. Drullinger, T.M. Fortier, J.E. Stalnaker, S.A. Diddams, W.C. Swann, N.R. Newbury, W.M. Itano, D.J. Wineland, J.C. Bergquist, Science **319**(5871), 1808–1812 (2008)
6. S. Schmid, A. Härter, J. Hecker Denschlag, Phys. Rev. Lett. **105**, 133202 (2010)
7. C. Zipkes, S. Palzer, C. Sias, M. Köhl, Nature **464**, 388 (2010)
8. A. Grier, M. Cetina, F. Orucevic, V. Vuletic, Phys. Rev. Lett. **102**, 223201 (2009)
9. W.G. Rellergert, S.T. Sullivan, S. Kotochigova, A. Petrov, K. Chen, S.J. Schowalter, E.R. Hudson, Phys. Rev. Lett. **107**, 243201 (2011)
10. K. Ravi, S. Lee, A. Sharma, G. Werth, S.A. Rangwala, Nat. Commun. **3**, 1126 (2012)
11. F.H.J. Hall, M. Aymar, N. Bouloufa-Maafa, O. Dulieu, S. Willitsch, Phys. Rev. Lett. **107**, 243202 (2011)

12. M. Harlander, M. Brownnutt, W. Hänsel, R. Blatt, New J. Phys. **12**, 093035 (2010)
13. S.X. Wang, G. Hao Low, N.S. Lachenmyer, Y. Ge, P.F. Herskind, I.L. Chuang, J. Appl. Phys. **110**, 104901 (2011)
14. N. Daniilidis, S. Narayanan, S.A. Möller, R. Clark, T.E. Lee, P.J. Leek, A. Wallraff, F. St. Schulz, F. Schmidt-Kaler, H. Häffner, New J. Phys. **13**(1), 013032 (2011)
15. N. Yu, W. Nagourney, H. Dehmelt, J. Appl. Phys. **69**(6), 3779–3781 (1991)
16. R.G. DeVoe, C. Kurtsiefer, Phys. Rev. A **65**, 063407 (2002)
17. S. Narayanan, N. Daniilidis, S.A. Möller, R. Clark, F. Ziesel, K. Singer, F. Schmidt-Kaler, H. Häffner, J. Appl. Phys. **110**(11), 114909 (2011)
18. D.T.C. Allcock, T.P. Harty, H.A. Janacek, N.M. Linke, C.J. Ballance, A.M. Steane, D.M. Lucas, R.L. Jarecki Jr., S.D. Habermehl, M.G. Blain, D. Stick, D.L. Moehring, Appl. Phys. B **107**(4), 913–919 (2012)
19. M. Debatin, M. Kröner, J. Mikosch, S. Trippel, N. Morrison, M. Reetz-Lamour, P. Woias, R. Wester, M. Weidemüller, Phys. Rev. A **77**, 033422 (2008)
20. D.J. Berkeland, J.D. Miller, J.C. Bergquist, W.M. Itano, D.J. Wineland, J. Appl. Phys. **83**(10), 5025–5033 (1998)
21. Q.A. Turchette, D. Kielpinski, B.E. King, D. Leibfried, D.M. Meekhof, C.J. Myatt, M.A. Rowe, C.A. Sackett, C.S. Wood, W.M. Itano, C. Monroe, D.J. Wineland, Phys. Rev. A **61**, 063418 (2000)
22. L. Deslauriers, S. Olmschenk, D. Stick, W.K. Hensinger, J. Sterk, C. Monroe, Phys. Rev. Lett. **97**, 103007 (2006)
23. J. Labaziewicz, Y. Ge, D.R. Leibrandt, S.X. Wang, R. Shewmon, I.L. Chuang, Phys. Rev. Lett. **101**, 180602 (2008)
24. D.T.C. Allcock, L. Guidoni, T.P. Harty, C.J. Ballance, M.G. Blain, A.M. Steane, D.M. Lucas, New J. Phys. **13**(12), 123023 (2011)
25. D.A. Hite, Y. Colombe, A.C. Wilson, K.R. Brown, U. Warring, R. Jördens, J.D. Jost, K.S. McKay, D.P. Pappas, D. Leibfried, D.J. Wineland, Phys. Rev. Lett. **109**, 103001 (2012)
26. F. Rossi, G.I. Opat, J. Phys. D Appl. Phys. **25**, 1349 (1992)
27. J.B. Camp, T.W. Darling, R.E. Brown, New J. Phys. **71**, 783 (1992)
28. A. Härter, A. Krükow, M. Dei B. Drews, E. Tiemann, J. Hecker Denschlag, Nat. Phys. **9**, 512–517 (2013)
29. A. Härter, A. Krükow, A. Brunner, J. Hecker Denschlag, Appl. Phys. Lett. **102**, 221115 (2013)
30. S. Schmid, A. Härter, A. Frisch, S. Hoinka, J. Hecker Denschlag, Rev. Sci. Instrum. **83**, 053108 (2012)